Shape recovery characteristics of biaxially prestrained Fe-Mn-Si-based shape memory alloy

Wada, Manabu
Naoi, Hisashi
Yasuda, Hidehiro
Maruyama, Tadakatsu

(Citation)
Materials Science and Engineering: A,481-482:178-182

(Issue Date)
2008-05

(Resource Type)
journal article

(Version)
Accepted Manuscript

(URL)
https://hdl.handle.net/20.500.14094/90001071

Shape recovery characteristics of biaxially-prestrained FeMnSi-based shape memory alloy

M. Wada[1], H. Naoi[1] and H. Yasuda[2]
[1]*Faculty of Engineering, Hosei University, 3-7-2 Kajino-cho, Koganei 184-8584, Japan*
[2]*Department of Mechanical Engineering, Kobe University, Nada, Kobe 657-8501, Japan*

TEL: ++81 42 387 6151 *FAX: ++81 42 387 6121*
E-mail: mwada_bb@ybb.ne.jp

Abstract

FeMnSi-based shape memory alloy has already been used practically as steel pipe joints. In most of the applications including the steel pipe joints, it is possible to estimate the reduction of diameter from the experimental data of the shape recovery after uniaxial stretching of the alloy materials. However, studies on shape recovery effects after biaxial stretching are important for the extensive applications of the alloy. In this study, we investigated the shape recovery strain after uniaxial and biaxial stretching and the microstructures of the alloy in order to see effects of uniaxial and biaxial prestrain on the stress-induced martensitic transformation. Amounts of shape recovery strain in the biaxially-prestrained specimens are smaller than those in the uniaxially-prestrained specimens. The TEM observations revealed that reverse transformations of stress-induced martensitic ε-phase are prevented by slip bands formed at the same time in the biaxially-prestrained specimens, but not in the uniaxially-prestrained specimens. The technological data and interpretation presented in this study should be useful in forming design guidelines for promoting the extensive applications of FeMnSi-based shape memory alloy.

Keywords: FeMnSi-based shape memory alloy, piping fabrications, biaxial prestrain, stress-induced martensitic transformation, orientation of ε-phase, ferrum-manganese-silicon

1. Introduction

FeMnSi-based shape memory alloy is expected to be utilized for piping fabrications [1,2] and structural members, and it has already been used practically as steel pipe joints [3]. In order to utilize the alloy to these applications, it is necessary to clarify relationship between prestrain and shape recovery strain. Prestrains are introduced in the alloy not only by uniaxial tension and compression but also by biaxial tension-tension and tension-compression. In many cases of the applications, shape recovery strains are estimated from the shape recovery effect under uniaxial prestrain [4]. However, to develop various fields of its practical applications, we need to estimate shape recovery strains under biaxial prestrain introduced in the alloy materials. From the background mentioned above, we have investigated shape recovery characteristics under uniaxial tensile prestrain, biaxial tensile prestrain, tensile-compressive prestrain, and prestrain mixed by uniaxial and biaxial tension. In addition, we observed the changes in microstructures of the alloy during the shape recovery by transmission electron microscopy (TEM).

In this study, we report on the shape recovery characteristics of uniaxially- and biaxially-prestrained FeMnSi-based shape memory alloy.

2. Experimental Procedures

2.1 Prestraining by uniaxial stretching and shape recovery

A plate consisting of Fe-28%Mn-6%Si-5%Cr (mass %) [5] was used as a specimen in this study. The plate was hot-rolled at 1423K to 0.8mm thick sheets. After rolling, solution heat treatment was conducted at 1223K for 1hour. Plastic anisotropy of the sheet was not observed. We firstly investigated the shape recovery strains of the specimens prestrained by uniaxial stretching, in order to clarify the shape recovery effect in uniaxially-prestrained specimens. The specimens of 200mm in length and 25mm in width were manufactured by machining from the sheet. Initial gage length of the specimens was set at 50mm. Longitudinal direction of the specimens was coincided with rolling direction of the sheet. After preparation of the specimens, the specimens were prestrained by uniaxial stretching in the longitudinal direction. The plastic strains were introduced in the range of 0 to 12% at intervals of 2%. After stretching, the changes in the gage length were measured by optical microscope. Table 1 shows the physical properties of specimens.

Table 1 Mechanical properties and transformation temperatures in Fe-28%Mn-6%Si-5%Cr shape memory alloy.

Properties	Longitudinal direction	Transversal direction
0.2% Proof stress $\sigma_{0.2}$ (MPa)	271	267
Tensile strength TS (MPa)	815	811
Total elongation $T\text{-}El$ (%)	38.6	37.9
Martensitic start temperature M_s (K)	253 ~ 298	
Austenitic finish temperature A_f (K)	403 ~ 458	

Prestrain in the longitudinal direction $\varepsilon_{p\ell}$ and that in the transversal direction ε_{pt} are defined as follows.

$$\varepsilon_{p\ell} = \ln(L_{2\ell} / L_{1\ell}) \quad (1)$$

$$\varepsilon_{pt} = \ln(L_{2t} / L_{1t}) \quad (2)$$

where $L_{1\ell}$ and $L_{2\ell}$ are the gage lengths before and after prestraining in the longitudinal direction, and L_{1t} and L_{2t} are those in the transversal direction, respectively.

Finally, the specimens were annealed at 673K for 600 seconds so as to recover the shapes. The shape recovery strain along the longitudinal direction $\varepsilon_{r\ell}$ and that along the transversal direction ε_{rt} were defined as follows.

$$\varepsilon_{r\ell} = \ln(L_{3\ell} / L_{2\ell}) \quad (3)$$

$$\varepsilon_{rt} = \ln(L_{3t} / L_{2t}) \qquad (4)$$

where $L_{2\ell}$ and $L_{3\ell}$ are the gage lengths before and after annealing in the longitudinal direction, and L_{2t} and L_{3t} are those in the transversal direction, respectively.

2.2 Prestraining by biaxial stretching and shape recovery

We firstly investigated the shape recovery strains of specimens prestrained by biaxial stretching. The specimens were squared by machining from the alloy sheet. The four sides were 200 mm in length. The surface of specimen was marked with circles of 5 mm in diameter by electrolytic corrosion. Initial gauge length of 20mm was set at the center of the specimens. Secondly, specimens were prestrained by bulge forming. Four kinds of dies were used for bulge forming. The shapes of the rim in the individual dies were round of 150mm diameter, oval 150 mm in length x 120 mm in width, oval 150 mm x 100 mm, and oval 150 mm x 75 mm termed type A, B, C, and D, respectively. The ellipticity k of the dies is defined as follows.

$$k = (L_D - W_D) / L_D \qquad (5)$$

where L_D and W_D are the length of major and minor axis in the elliptical rim, respectively. The ellipticity k in the type A, B, C, and D were calculated to be 0, 0.2, 0.33, and 0.5, respectively.

Major axis of the bulge shape was coincided with rolling direction of the alloy sheet. Pressure for bulge forming was set from 2MPa to 20MPa at intervals of 2MPa. After bulge forming, changes in gage lengths were measured by optical microscope. The prestrain in the longitudinal direction $\varepsilon_{p\ell}$ and that in the transversal direction ε_{pt} were calculated by formulae (1) and (2), respectively. The specimens after bulge forming are shown in figure 1, and experimental conditions of bulge forming are shown in table 2.

Finally, the specimens were annealed at 673K for 600 seconds so as to recover the shapes. The shape recovery strain in the longitudinal direction $\varepsilon_{r\ell}$ and that in the transversal direction ε_{rt} were calculated by formulae (3) and (4), respectively.

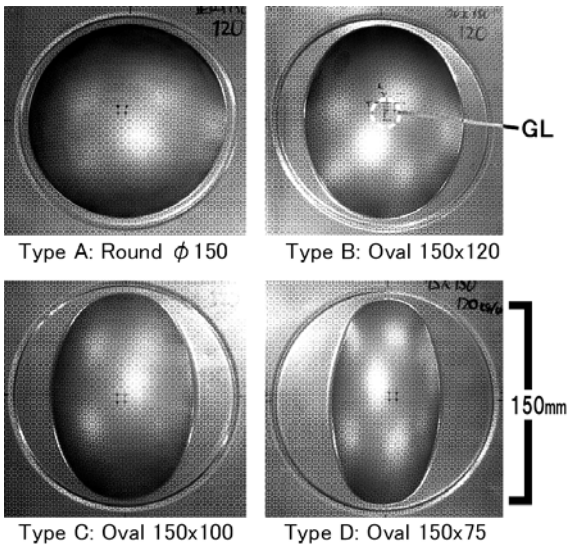

Fig. 1 Specimens after bulge forming at 12MPa.

Table 2 Experimental conditions of bulge forming.

Type	Bulge shape (mm)	Ellipticity k	Bulging pressure (MPa)
A	Round ϕ 150	0	2, 4, 6, 8, 10, 12, 14, 16
B	Oval 150 x 120	0.2	2, 4, 6, 8, 10, 12, 14, 16
C	Oval 150 x 100	0.33	2, 4, 6, 8, 10, 12, 14, 16
D	Oval 150 x 75	0.5	2, 4, 6, 8, 10, 12, 14, 16

2.3 Microstructural observations by TEM

In order to study the microstructural changes during shape recovery, the uniaxially- and biaxially-prestrained specimens were subjected to in situ annealing experiments in a TEM. The TEM specimens were prepared by sequential mechanical polishing of the prestrained sheets, cutting from the sheet to discs of 3 mm diameter, followed by electrolytic polishing in the solution consisting of methanol and nitric acid to electron transparency. The microstructures of the specimens were observed by bright-field images (BFIs) and selected area electron diffractions (SAEDs). The microscopes used were Hitachi H-800, operating at accelerating voltages of 200kV.

3. Results

3.1 Relationship between prestrain and shape recovery strain

Relationship between prestrain and shape recovery strain in the uniaxially- and biaxially-prestrained specimens is shown in figure 2. The shape recovery strains in the longitudinal direction $\varepsilon_{r\ell}$ are plotted as a function of the prestrain in the longitudinal direction $\varepsilon_{p\ell}$. The values of the shape recovery strain are denoted by negative values. In the uniaxially-prestrained specimens, the prestrain $\varepsilon_{r\ell}$ increases to the maximum value of −2% at 6% $\varepsilon_{p\ell}$, and then decreases slightly with increasing prestrain $\varepsilon_{p\ell}$. The slight reduction of $\varepsilon_{r\ell}$ above 6% $\varepsilon_{p\ell}$ may be attributed to the slip bands generated by greater deformation, since it is known that the maximum volume fraction of the stress-induced martensite phase is approximately 30% in the alloy [6].

On the other hand, in the biaxially-prestrained specimens, the values of $\varepsilon_{r\ell}$ slightly reduce in all of the types of A to D with increasing $\varepsilon_{p\ell}$. The shape recovery strain in the biaxially-prestrained specimens is smaller than that in the uniaxially-prestrained specimens by a factor from 1/4 to 1/2. Though the apparent differences in the four types of specimens are not recognized, the average values of $\varepsilon_{r\ell}$ in the range of the $\varepsilon_{p\ell}$ measured in the experiments become large with increasing the ellipticity of dies.

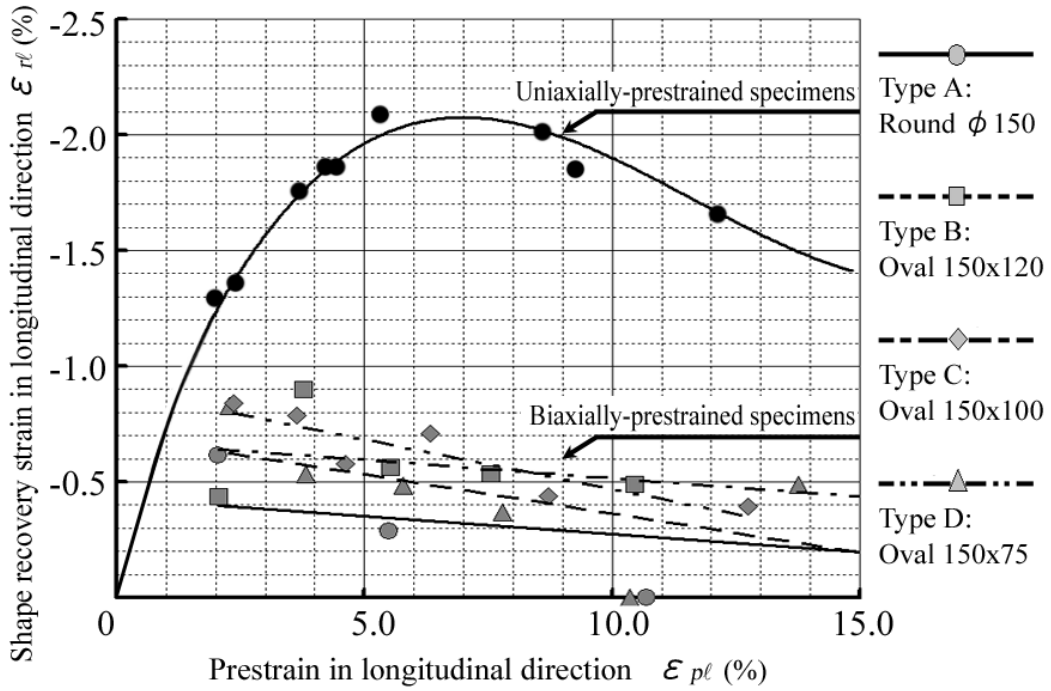

Fig. 2 Shape recovery strain in the longitudinal direction as a function of prestrain.

3.2 Hystereses of shape recovery strains in prestrained specimens

The hystereses of shape recovery strain in the uniaxially- and biaxially-prestrained specimens are shown in figure 3. The strain in the transversal direction is shown as a function of that in the longitudinal direction. The solid and block arrows indicate the changes in amounts and directions of shape recovery strains, that is vectors of shape recovery strains. The start-points and end-points of the arrows show values of strains before and after shape recovery in the prestrained specimens, respectively. When the uniaxial prestrains are loaded to the specimens, ε_{pt} is proportional to $\varepsilon_{p\ell}$, where the proportionality constant is approximately -0.5, since the volume is kept in constant and isotropic mass flow takes place in the transversal and thickness directions during the deformation by martensitic transformation in the alloy. All of the hystereses of the shape recovery strains are toward the origin along a line satisfied the equation ε_{pt}=-0.5$\varepsilon_{p\ell}$. On the other hand, when the biaxial prestrain is given in the specimens, ε_{pt} is again proportional to $\varepsilon_{p\ell}$, where the proportionality constant is approximately 1-k (k: the ellipticity of dies). In the small biaxially-prestrained specimens, hystereses of the shape recovery strains are toward the origin along the lines satisfied the equations ε_{pt}=(1-k)$\varepsilon_{p\ell}$, but in the large biaxially-prestrained specimens, they tend to be toward random directions.

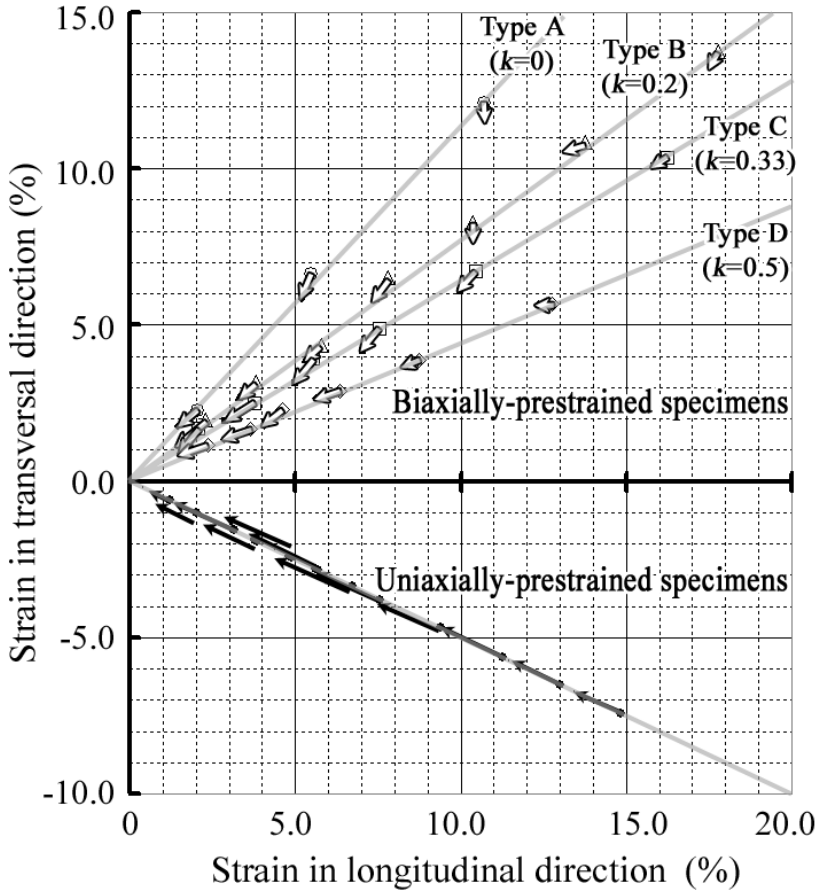

Fig. 3 Hysteresis of shape recovery strain in the uniaxially- and biaxially-prestrained specimens.

3.4 Microstructural changes during annealing in the uniaxially- and biaxial-prestrained specimens

Figures 4(a) and (b) show the BFIs from the same area in the 1% uniaxially-prestrained specimens before and after annealing at approximately 600 K, respectively. In Fig. 4(a), the contrasts from the second phase along a <110> direction are recognized in the γ matrix phase. The second phase was identified as the ε-phase which has the hcp structure by SAEDs. The ε-phase in each grains is observed along only one of the <110> directions. In Fig. 4(b), most of the contrasts from the second phase disappear, but the strain contrasts from dislocations on one kind of the slip band remain even after annealing. It was revealed from Fig. 4 that the ε-phase and slip bands formed by uniaxial tensile prestrain are oriented along only one kind of crystalline direction in the grain, and the ε-phase can disappear without barrier after annealing.

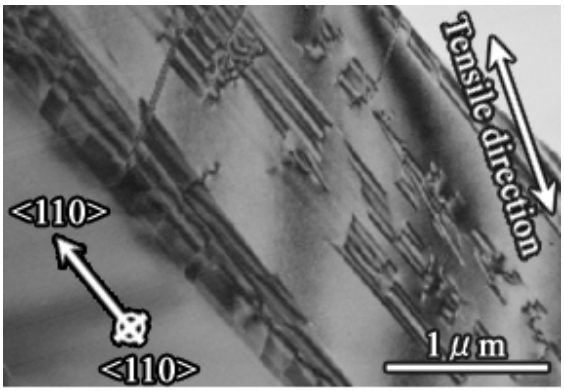

(a) 1% uniaxially-tensile prestrained specimen before annealing.

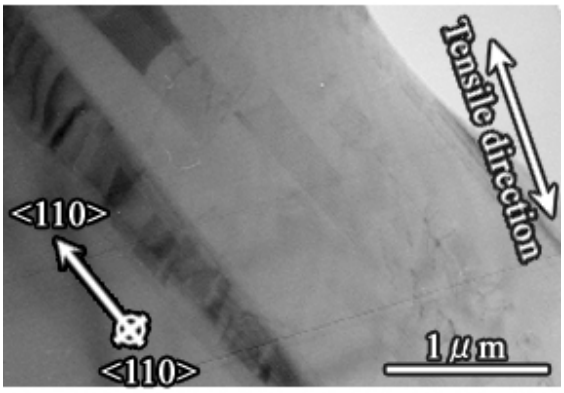

(b) 1% uniaxially-tensile prestrained specimen after annealing.

Fig. 4 BFIs from 1% uniaxially-tensile prestrained specimens. (a) before and (b) after annealing at approximately 600 K.

Figures 5(a) and (b) show the BFIs from the same area in the 1% biaxially-prestrained specimens before and after annealing at approximately 600 K, respectively. In Fig. 5(a), the microstructure in the grain is complicated as compared with that in Fig. 5(a). The single and double arrows indicate ε-phase and slip bands, respectively. Both contrasts of ε-phase and slip bands appeared along three different <110> directions cross each other. In Fig. 5(b), not only the contrasts from the slip bands are recognized but also those from the ε-phase. It was revealed from Fig. 5 that the complete disappearance of the ε-phase are prevent by the pinning interaction between the ε-phase and slip bands formed at the same time along the multiple directions in the grain.

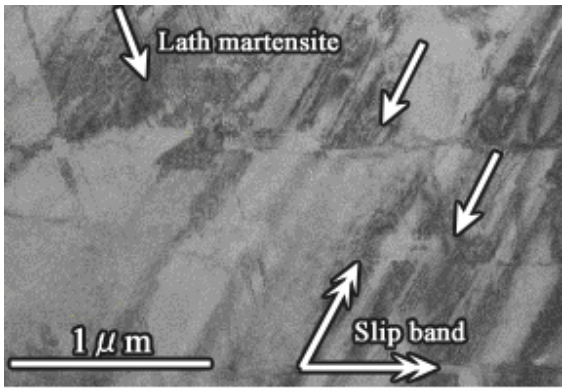

(a) 1% biaxially-tensile prestrained specimen before annealing.

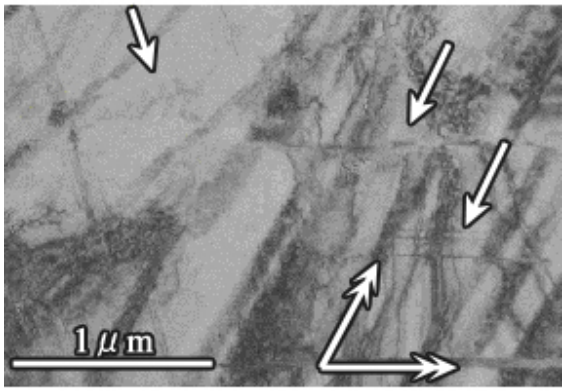

(b) 1% biaxially-tensile prestrained specimen after annealing.

Fig. 5 BFIs from 1% biaxially-tensile prestrained specimen. (a) before and (b) after annealing at approximately 600 K.

4. Discussion

From the results, it was evident that the amounts of shape recovery strains in the biaxially-prestrained specimens are smaller than those in the uniaxially-prestrained specimens. All of the hystereses of the shape recovery strains are toward the origin along a line in the uniaxially-prestrained or small biaxially-prestrained specimens, but hystereses of the shape recovery strains tend to be toward random directions in only the large biaxially-prestrained specimens.

It is well-known that shape recovery characteristics of FeMnSi-based shape memory alloy depend on the martensitic transformation from γ- to ε-phase, which is induced by formation of a pole dislocation and multiplication of the partial dislocations on every alternate {111} plane [7]. In the uniaxially-prestrained specimens, the martensitic transformation takes place on the {111} plane, on which the value of Schmidt factor becomes maximum in individual grains and consequently the most favorably oriented ε-phase will be formed in a grain. The {111} planes on which the ε-phase is formed will be equivalent to those on which the subsequent slip bands are formed. During the shape recovery by annealing, reverse transformation from ε- to γ-phase simultaneously takes place without barrier in individual grains and the consequent large amounts of shape recovery strain are induced. On the other hand, the formation of the ε-phase

and slip bands will take place on the different multiple {111} planes in the biaxially-prestrained specimens, because it is difficult that the {111} planes on which the value of Schmidt factor becomes are restricted maximum in individual grains. When the ε-phase is pinned by crossing with the slip bands and the consequent reverse transformations in the ε-phase on the different {111} planes take place at random, the hystereses of the shape recovery strains may be considerably small and isotropic, particularly under the large biaxial prestrain.

5. Conclusions

We have investigated the shape recovery characteristics of FeMnSi-based shape memory alloy under uniaxial and biaxial tensile prestrain, and have observed microstructural changes during the shape recovery in the alloys by TEM. In both of them, the hysteresis lines of the shape recovery strains are along the same lines with those of the prestrains. Meanwhile, amounts of shape recovery strains in the biaxially-prestrained specimens are smaller than those in the uniaxially-prestrained specimens. The TEM observations revealed that reverse transformations of stress-induced martensitic ε-phase are prevented by slip bands formed at the same time in the biaxially-prestrained alloys, but not in the uniaxially-prestrained alloys.

References

[1] M. Wada, K. Narita, H. Naoi and T. Maruyama, Proc. of TMP'2004 (2004) pp.1-8.
[2] Y. Joto, M. Wada, H. Naoi and T. Maruyama, Proc. of IMECE2004 (2004) pp.1-5.
[3] T.Maruyama, T.Kurita, Kinzoku 74 (2004) pp.48-51.
[4] M. Wada, H. Naoi and K. Tsukimori, Proc. of IMECE2003 (2003) pp.1-6.
[5] H. Otsuka, H. Yamada, T. Maruyama, H. Tanahashi, S.Matsuda and M. Murakami, ISIJ Int., 30-8 (1990), pp.674-679
[6] H. Otsuka, H. Murakami and S. Matsuda, Proc.of MRS Int. Mtg. on Advanced Materials, 9 (1989) pp.451-456
[7] A.Sato, H. Kubo and T.Maruyama, Mater. Trans. 47-3 (2006) pp.571-579